Iranian Journal of Chemical Engineering

Journal Homepage: www.ijche.com

pISSN: 1735-5397
eISSN: 2008-2355

Regular Article

Prediction of Erosion Rate in Gas-Solid Flow Using Computational Fluid Dynamics (CFD): Focus on Geometrical Parameters

***K. Jalalvandi*[1], *A. Parvareh*[1,2*]**

[1] *Faculty of Petroleum and Chemical Engineering, Razi University, Kermanshah 6714967346, Iran*
[2] *CFD Research Group, Advanced Chemical Engineering Research Center, Faculty of Petroleum and Chemical Engineering*

ARTICLE INFO

Article history:
Received: 2023-06-28
Accepted: 2023-09-23
Available online: 2023-09-23

Keywords:
Erosion,
Fluid flow,
Solid particles, Modelling,
Corrosion,
CFD,
COMSOL

ABSTRACT

In this study, the fluid flow together with solid particles has been studied using Computational Fluid Dynamics (CFD). The gas-solid flow (air and sand particles with the size of 150 µm) inside a 76.2 mm diameter pipe with various bend angles including 45, 60, 90, 120, 135, and 180° was modelled at the fluid flow velocity of 11 m/s. The k-ω turbulence model was employed to model the flow turbulence and the E/CRC erosion model have been used to predict erosion rates. The hydrodynamics of the flow, the particles motion as well as the probable erosion regions were predicted. The CFD simulation results showed that increasing the curvature angle increases the erosion rate. While, increasing the pipe diameter, decreases the erosion rate. The maximum erosion rate was predicted at the end part of the curvature for 45 and 60 ° angles, while it was observed in the middle region for 120 and 135 ° curvatures. Finally, the maximum erosion rate for the 180 ° curvature was observed in two regions at the end of the first and second half. Using these results, precautionary considerations for the erosion, and the suitable plans for the repair and maintenance of the equipment can be offered.

DOI: 10.22034/ijche.2023.402980.1495 URL: https://www.ijche.com/article_179917.html

1. Introduction

Sand particles are inherently present in the extracting and delivering raw materials in the engineering industry. These particles cause several problems related to the flow assurance [1]. The flow dynamics in pipes are very

*Corresponding author: a.parvareh@razi.ac.ir, (A. Parvareh); arsalanparvareh@yahoo.com

complex systems because they are strongly influenced by flow conditions [2]. The pipeline erosion is caused by solid particles impinging on the inner surface walls of the pipeline during production. As a result, the oil and gas industry lose many millions of dollars each year. Failures in pipelines, particularly elbows that change flow directions, are largely caused by particles that travel across flow streamlines and impact bends in high-flow pipelines.[3]. Several industries and research centers are interested in Tools that can be used to identify and resolve this problem. For the prediction of the component failure, it is essential to obtain an efficient method of determining erosion. Furthermore, engineers can use accurate erosion predictions to determine the service life of equipment and to identify areas where significant erosion might happen [4]. Shale gas gathering and transportation pipelines are susceptible to erosion-corrosion damages at 90° elbows [5]. In general, There are three types of studies for the prediction of erosion : experimental studies, numerical simulations, and the development of erosion models [6]. Due to the complexity of the multiphase flow erosion, researchers have conducted experiments and obtained data on the location and rate of erosion in 90° elbows. Ultimately, this information can be used to develop models to predict erosion and validate simulations based on the computation of fluid dynamics (CFD) [7].

Top research institutions have been using the computational fluid dynamics analysis to estimate pipeline erosion rates in recent years [8]. A COMSOL simulation was used to study the erosion of natural gas and oil pipelines [9]. There are three components to this comprehensive process: the simulation of flow, particle tracking, and erosion calculations. [10]. The CFD analysis with the Eulerian-Lagrangian approach calculates the continuous phase using Navier-Stokes equations, while the secondary phase is determined by the particle force balance. For more accurate results, the Reynolds Stress Model with a low Reynolds number correction is used to model the turbulent behavior of the continuous fluid phase at the near wall region and secondary flows at the elbow.[11]. Next, a review of previous erosion studies is presented.

Viera et al. presented a comprehensive modeling and computational study that evaluates erosion because of sand particles in airflow on elbow. In this research, the identification of the erosion in a standard bend was successful. The area of the maximum erosion was determined for single-phase (gas) flows with sand at about 45° to the bend. In single-phase flows, by increasing the particle size, the area of maximum erosion rate did not change. The 300mm sand produced 1.9 to 2.5 times higher erosion rates than the 150mm sand due to its sharper edge. The erosion rate increases by increasing the gas velocity.[12]

In another study, Bilal et al performed an experimental investigation of 45° and 90° bends and the different effects of the radius of the pipe curvature on the erosion rate of solid particles. By changing the bend direction from 90° to 45°, the erosion rate is also reduced. According to the experimental results, the color was removed from all elbows at the end of their bent exit.[3]

Jia et al. developed a laboratory device for evaluating the erosion-corrosion characteristics of a 90° steel bend in a three-phase flow. Additionally, based on the Fluent code, a numerical simulation model was developed in order to forecast erosion-corrosion characteristics. Experiments and simulations showed that the most significant erosion-corrosion region of the pipe bend is between -45° and 45° radial angles and between 20° and 50° axial angles.[5]

In this study, Computational fluid dynamics (CFD) has been used to study the fluid flow with solid particles. The purpose of this study is to evaluate the effect of the pipe elbow geometry on flow variables and the erosion rate prediction by using Reynolds Averaging Navier- Stokes (RANS) coupled with Particle Tracing Modeling (PTM). A computational platform based on COMSOL Multiphysics was used to accomplish the research objectives and goals.

2. CFD simulation

2.1. Simulation geometries and Meshing

This research is focused on the flow inside process pipelines, so the flow containing solid particles has been simulated within a section of the pipeline. A stainless steel 316 (SS316) Pipe having an internal diameter of 3 in (76.2 mm) and a bend radius of 1.5 D (114.3 mm) in two vertical and horizontal orientations was modeled. The straight lengths of 1000 and 600 mm were considered before and after the bend respectively. Several bend angles including 45°, 60°, 90°, 120°, 135° and 180° for the external angle were examined in the simulation. Figure 1 shows the geometry of the studied bends. It should be noticed that the bend angle is named according to the complementary angle of the bend opening angle.

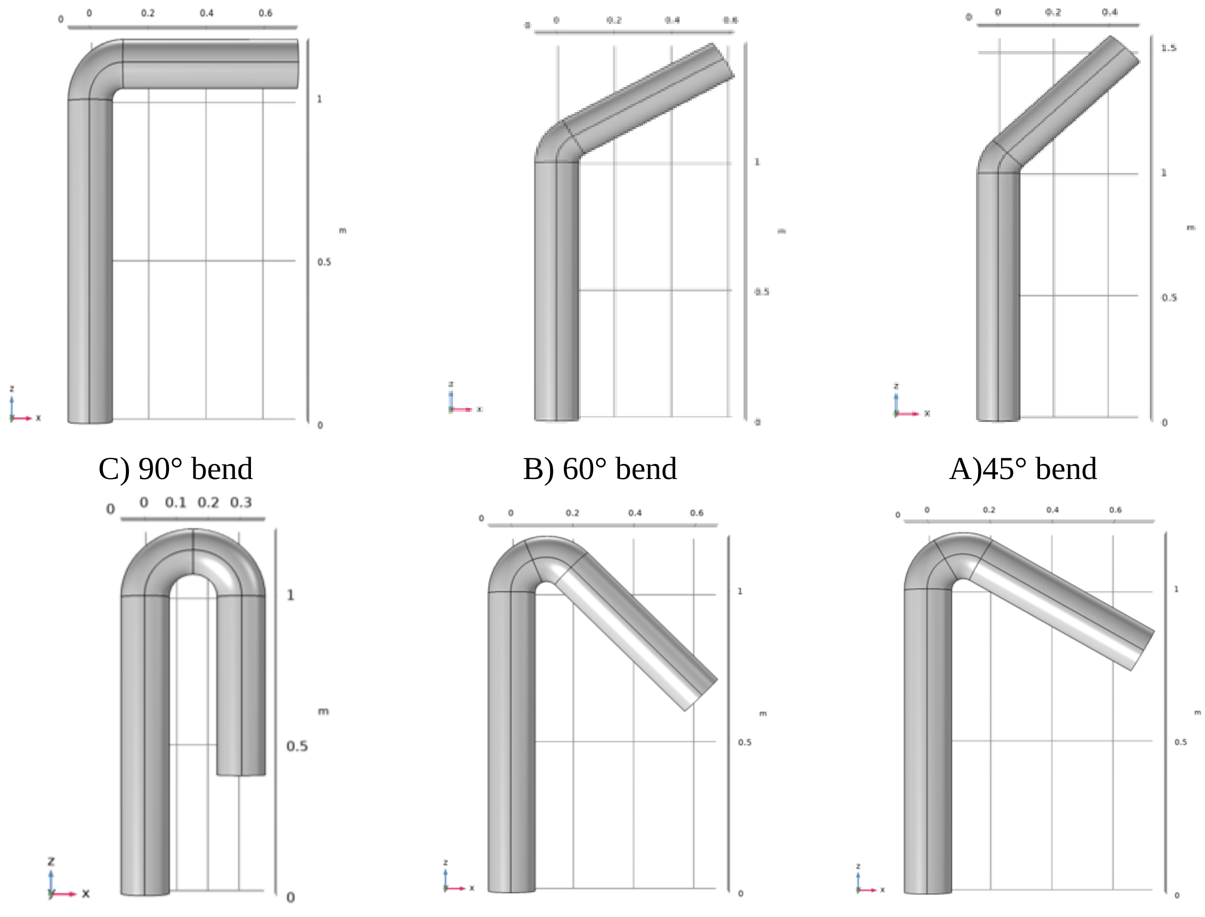

C) 90° bend B) 60° bend A)45° bend

F)180° bend E) 135° bend D)120° bend

Figure 1. Geometrical schematic of the considered bends for the simulation

Geometry meshing is essential for performing an accurate calculation and reducing the time of the calculation. there are three types of meshing used in the simulation using the computational fluid dynamics technique: unstructured (unorganized), structured (organized), and combined. Unstructured meshes are easier to generate, but their accuracy is disputed. In sensitive areas or curves, especially at the wall boundary, structured meshing provides greater accuracy than unstructured meshing. Creating boundary layers at wall boundaries is useful for meshing and flow calculations at bends and adjacent walls. This meshing strategy overcomes the limitations and disadvantages of the unstructured meshing, this meshing method is effective for a variety of applications involving computational fluid dynamics. In this study, structured meshes were created in order to reduce the computation time and to improve accuracy.

the generated mesh for the 90° bend is shown in figure 2. A triangular mesh was used for the pipe and a quadrilateral dominant mesh was created by using the sweeping method in the remaining domain. The mesh size was considered smaller in the bend as a sensitive area.

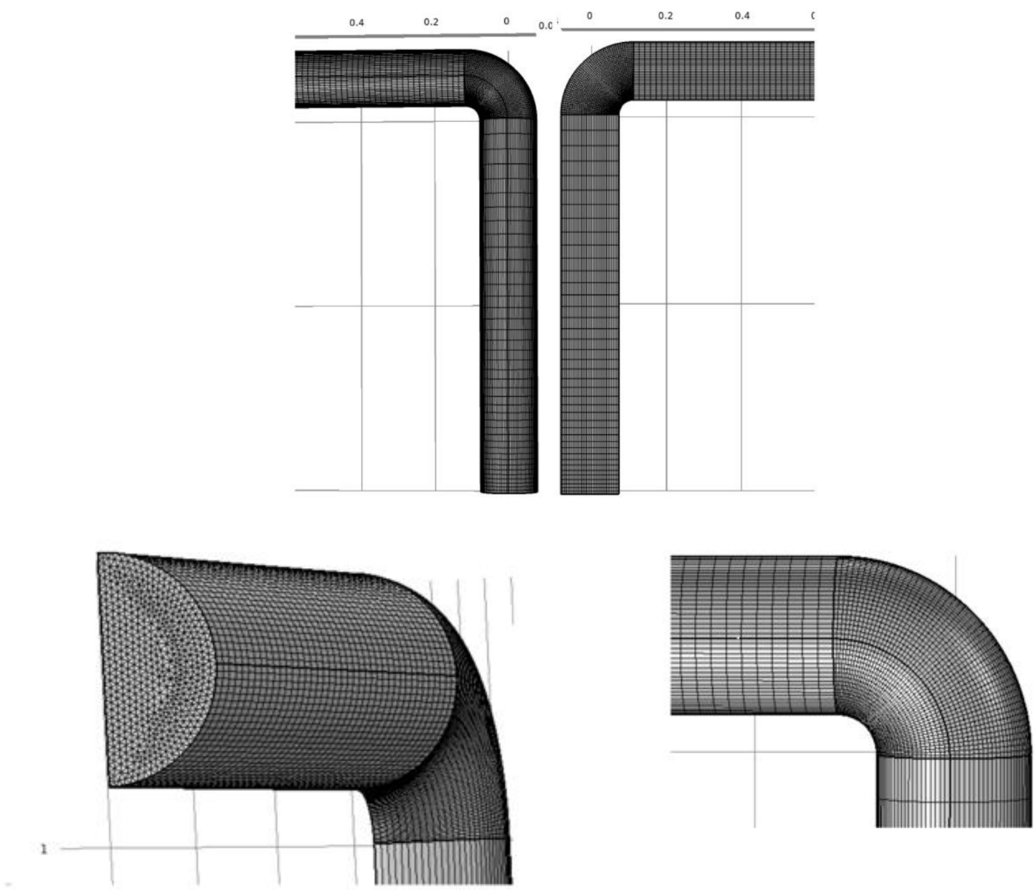

Figure 2. Generated meshes for the 90° bend

2.2. Applying governing equations

In this study, the air flow and the solid particles of the sand have been considered as the continuous and discrete phases consequently. The air flow with certain fractions of solid particles enters at the inlet with predefined velocities. The conservation equation including the mass and momentum, has been applied for the fluid flow. Reynolds number of the flow, considering the pipe diameter, the physical properties of the fluid and the velocity of the flow, is equal to 53000, which indicates a turbulent flow in the pipe. Since the erosion rate is determined based on wall collisions, a turbulent model, that can provide reliable predictions of parameters at the boundaries of the walls, must be selected.

In this research, a two-equation k-ω turbulence model has been used for the continuous phase turbulent flow. This flow model predicts the flow characteristics around high curvature regions more accurately based on the pipe curvature[13].

Newton's second law deals with the solid particles' motion, it differs from the Navier-Stokes equation for the fluid flow. A particle with a certain mass subjected to different forces is described by Newton's second law as follows[14]:

$$\frac{\mathrm{d}\left(m_{\mathrm{p}}V\right)}{\mathrm{d}t} = F_{\mathrm{D}} + F_{\mathrm{G}} + F_{\mathrm{ext}} \qquad (1)$$

In which, F_{ext}, F_G, and F_D denote the external, gravitational, and drag forces, respectively. V and m_p indicate the particle speed (m/s) and particle mass (kg).

Previous studies have used a variety of models to predict the erosion rates in particle-wall contacts. These models are empirically obtained based on fundamental concepts and objective functions, but differ in their application.

There are various models, including Finnie[15], E/CRC, OKA[16], and DNV[17] models, to predict erosion rates. These models are based on a variety of variables and constants derived from experimental data. In this study, the E/CRC erosion model has been used to predict erosion rates and identify possible leakage points on the pipe surface[18]. E/CRC model variable descriptions and empirical values are presented in Table 1.

Table 1
Parameters of the particle tracing Physics

physics	Parameter	Input
Particle tracing	Formulation	Newtonian
	Turbulent dissipation model	Discrete random walk
	Drag law	Stokes
	Erosion model	E/CRC
	Particle interaction force	Coulomb
	E/CRC model coefficient, C	7e-5.17
	Brinell hardness of surface material, BH	217
	Particle shape coefficient, Fs	0.5
	E/CRC model exponent, n	2.41

2.3. Properties of materials

In this research, air and sand particles were considered as the continuous and dispersed phases. The properties of these materials as well as the pipe wall are presented in table 2.

Table 2
Properties of materials considered in the simulation

Material	Parameter	input
Air	Density	1.293kg/m^3
	Dynamic viscosity	1.81e-5 kg/(m.s)

Sand	Density	2650 kg/m^3
	Diameter	0.0015 m
	Shape factor	0.5
Stainless steel	Density	7990 kg/m^3

2.4. Boundary conditions

Defining appropriate boundary conditions based on desired physical conditions is an important part of a CFD simulation, due to the fact that the solution of the fluid flow equations depends on the definition of initial conditions and boundary conditions in the domain of solution.

The flow velocity (11 m/s) and atmospheric pressure were considered at the inlet and outlet of the pipe. Additionally, the walls were bounced, and the condition of no-slip is applied to the walls. The symmetry boundary condition was applied in all considered geometries to reduce the computational time.

The flow rate of solid particles at the pipe inlet was 0.0029 kg/s and its initial distribution was based on meshing when particles first entered the pipe. The exit and side wall condition was regarded as the bounce condition.

Moreover, the drag force, particle interaction force, and gravity force were considered for the entire solution domain.

3. Modelling Results and discussion

3.1. Grid independency Check

To verify the accuracy of calculations and the time required to perform them, we will reduce mesh size or increase the element number, until the accuracy of the solution has not changed significantly and only the time of computation increases with an increase in the number of elements. In this research, six mesh sizes (six numbers of elements) were considered for a 90° elbow. With regard to the different numbers of elements, the mesh quality and the maximum erosion rate were evaluated. These results are presented in table 4. The results illustrate that by increasing the number of elements from mode 1 to 5, noticeable changes for the average element quality and the erosion rate have been observed. While, changing the mesh size from mode 5 to mode 6, considerable changes to these parameters have not been made. But only a noticeable increase in the calculation time has been observed. As a result, the mesh of mode 5, which has the number of elements equal to 139360, has been selected as the optimal mode, and subsequent calculations are based on this number of elements.

Table 4

The results of the grid independency check for 90° elbow

mesh	1	2	3	4	5	6
Number of elements	5310	6840	19800	54860	139360	253500
Average element quality	0.8302	0.8276	0.8724	0.8738	0.8903	0.8941
Maximum erosion rate[mm/yr]	5.66	8.06	5.77	7.19	7.29	7.31

Figure (3) shows the change in the maximum erosion rate inside the knee according to the number of meshes. The diagram illustrates that with larger mesh sizes, the erosion rate was calculated with the fluctuating behavior, i.e., by changing the mesh, different erosion rates were obtained. As the mesh size was reduced, it was observed that the erosion rate converged to a specific number. Based on the observation if the mesh number exceeds a certain value, the changes in the erosion rate are very small, and only the calculation time increases. Due to the limitations of the solving time and computational cost, state 5 in table (1-4) was chosen as the appropriate mesh number.

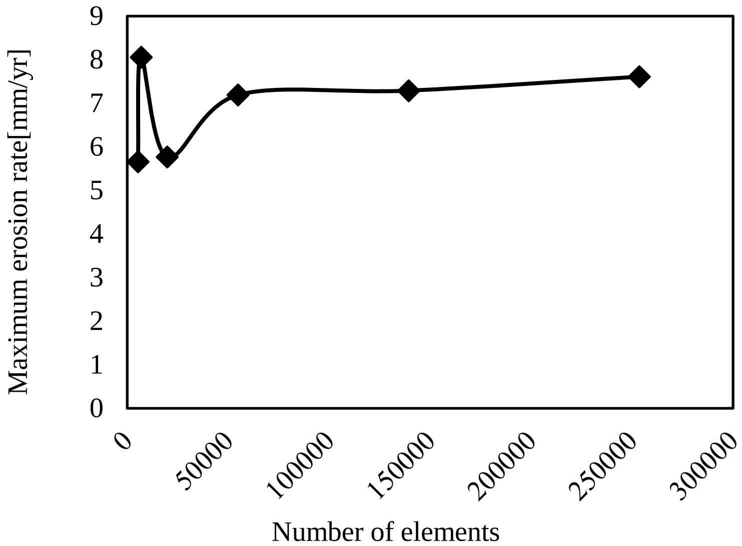

Figure 3. Changes in the erosion rate as a function of the mesh size

3.2. Validation of modelling results

To verify CFD simulation results, a comparison was made between the maximum predicted erosion rate for the 90° bend and the experimental results obtained by Vieira et al. under the same conditions[19]. As their experimental study, four inlet velocities of 11, 15, and 23 m/s and two particle sizes of 150 and 300 µm were considered in the simulation. The comparison of the predicted erosion rate with the experimental erosion rate at various considered velocities of the inlet flow as well as different particle sizes of the solid are presented in table 3. As it can be seen, an acceptable error is observed between the predicted and experimental erosion rates. For the smaller particles (150 µm) the obtained error is lower. The maximum error is observed in mode 4, which equals 36%.

Table 3

Predicted erosion rates compared to experimental erosion rates

case number	Vgas	Sand rate	Sand size	Max UT experiment rate	Max predicted erosion rate	Error
#	[m/s]	[kg/day]	[µm]	[mm/yr]	[mm/yr]	%
1	11	254	150	6.5	7.29	12
2	15	237	150	13.2	12.1	8
3	23	257	150	36.2	31.8	12
4	11	288	300	16.9	10.7	36
5	15	103	300	14.7	12.7	13
6	23	227	300	80.3	92.3	15

3.3. Hydrodynamics of the flow in the channel

The fluid velocity distribution as a part of the hydrodynamics of the flow, provides a comprehensive insight into the erosion behavior under prevailing environmental conditions. Figure 5 shows the predicted velocity contours for the considered geometries at a gas inlet velocity of 11 m/s.

In all of the cases, the flow which enters from the lower section of the pipe, has a uniform velocity distribution along the vertical portion of the pipe before entering the bend. There is a similarity between the distributions in modes 1 to 6. The uniform flow changes its behavior when it reaches the bends and a different distribution of the flow is observed at the inner and outer ends of each bend. All bends showed this change in behavior, and the higher speed of the flow is evident in the intrados of all bends. During the passage of the flow through the intrados of the bend, it makes a jump and separates from the wall. It then deviates towards the extrados of the bend and strikes it. The difference between the flow separation and its collision with the opposite wall at the outlet of the bend varies depending on the case, which results in different behavior of the erosion phenomenon.

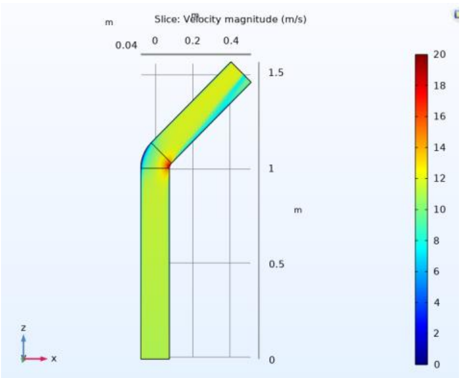

a) 45° bend

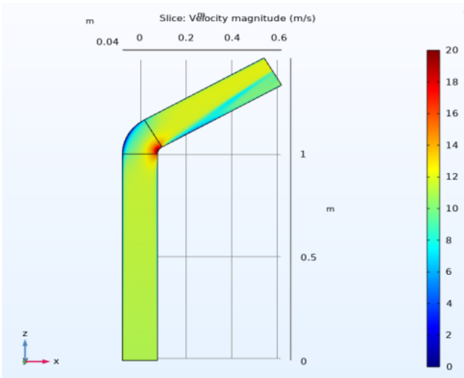

b) 60° bend

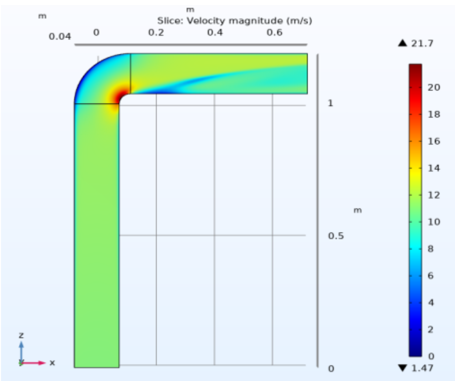

c) 90° bend

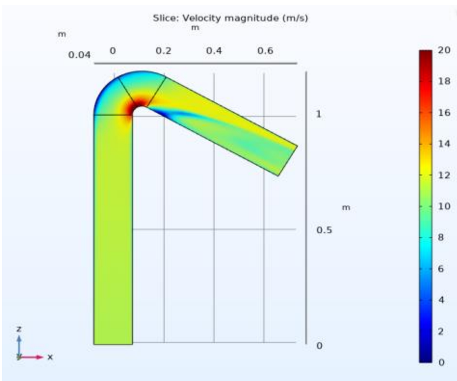

d) 120° bend

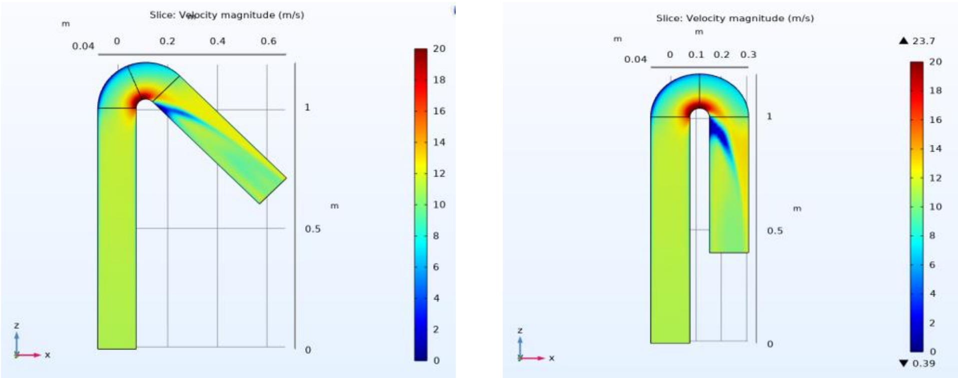

e) 135° bend f) 180° bend

Figure 4. Velocity distribution inside different bends for an inlet velocity of 11 m/s

3.4. Particle trajectory analysis

A flow containing solid particles is greatly influenced by the particle movement, and the collosion of dense mass particles on the wall causes erosion and destruction over the long time. Therefore, it is necessary to analyze the particle movement from the initiation of the flow until the quasi-steady behavior which has been achieved. A significant result of this simulation is the ability to analyze the solid particle movement in the fluid and predict the erosion rate. As an example ,Figure 5 illustrates the movement of particles in a fluid flow under a 90° bend angle over time (from the beginning of the particle injection until reaching a quasi-steady state) for a particle size of 150 μm and a particle rate of 0.00294 kg/s. the interaction between particles in the forms of particle-particle interaction, and fluid-particle interaction has been included in the simulation to track the particle movement in the pipe by incorporating the effect of the fluid path.

t=0.08s t=0.1s t=0.12s

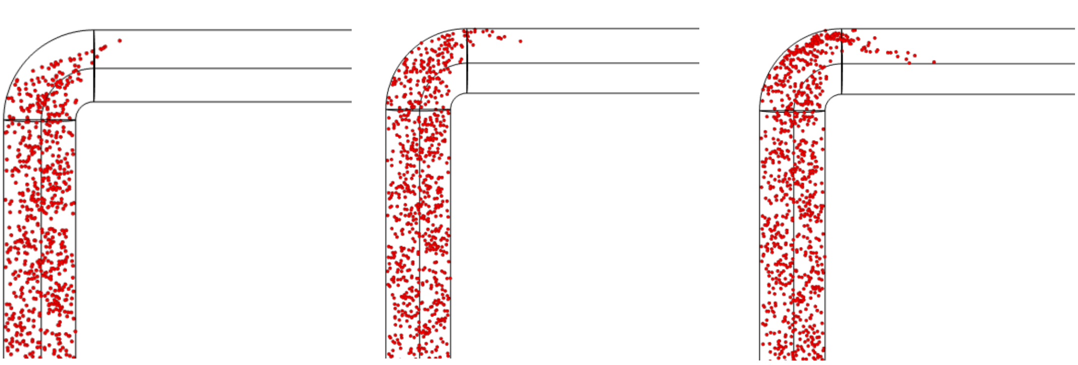

t=0.14s t=0.16s t=0.18s

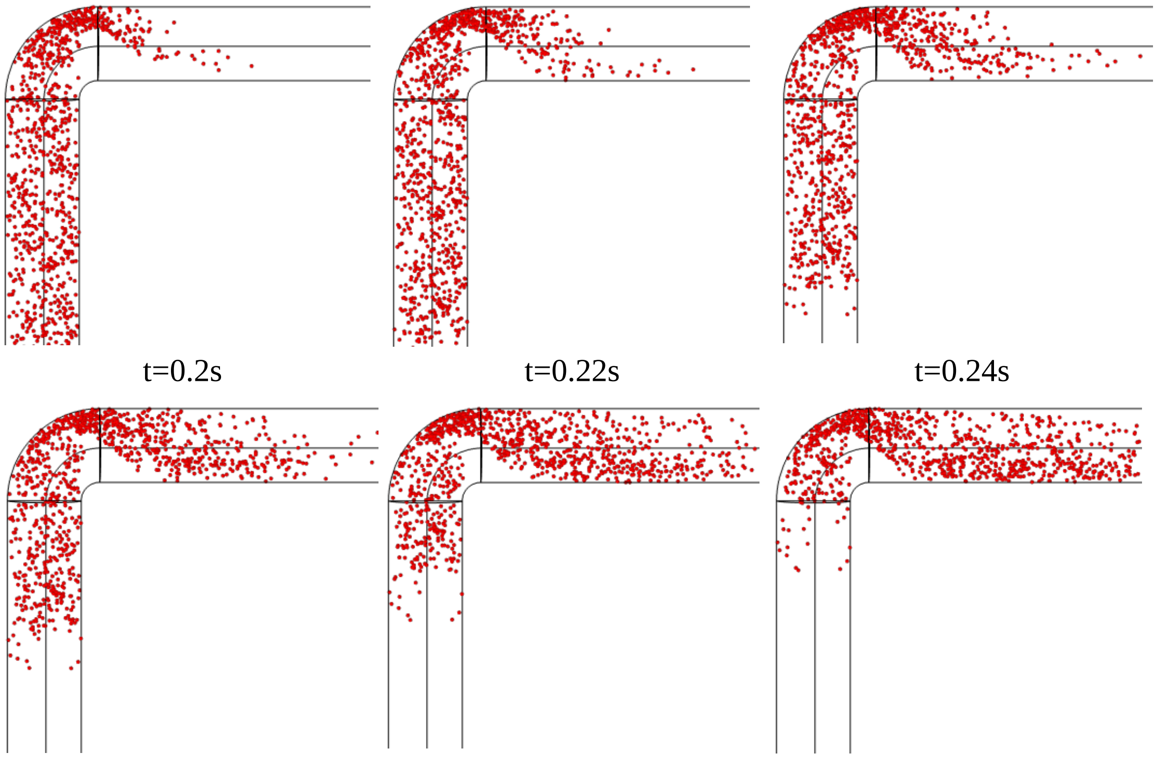

Figure 5. Movement path of the solid particles in the 90° bend at different times

3.5. Analysis of the parameters affecting the erosion rate

Parameters affecting the erosion rate include those related to the fluid flow, solid particles as well as the geometry and material of the surface exposed to the flow. By examining these parameters and their effects on the erosion rate, we can get a clearer understanding of this issue, this may reduce the erosion rate and the cost of equipment maintenance. In the present study, it has been focused on the geometrical parameter of the channel including the pipe diameter, bend angle as well as pipe orientation. An analysis of the effects of the stated parameters on erosion rates is provided in this section.

3.5.1. Pipe diameter

In order to investigate the parameters related to the geometry of the pipe on the erosion rate, the effect of the two parameters of the pipe diameter and pipe angle has been studied in the CFD simulation. Figure 5 shows the effect of the pipe diameter on the maximum erosion rate in a 90° elbow for the particle diameters of 76 to 250 mm, an inlet velocity of 11 m/s, and a particle rate equal to 0.00294 kg/s. Simulation results indicate that the erosion rate decreases rapidly by increasing the pipe diameter and reaches a very low level at a pipe diameter of 250 mm. the maximum erosin rate for the pipe diameter of 100 mm is twice the same quantity for the pipe diameter of 250 mm. The reason for this reduction in the erosion rate is that a pipe with a larger diameter has a larger contact surface and, as a result, the density of impacting particles per unit area is reduced. Therefore, this decrease in the particle density per unit area causes the reduction in the rate of particles hitting that surface, and consequently, the erosion rate decreases. An equation with a power of -1.87 for the pipe diameter was derived by the regression of the simulation data, indicating a sharp decrease in erosion rate with an increase in pipe diameter.

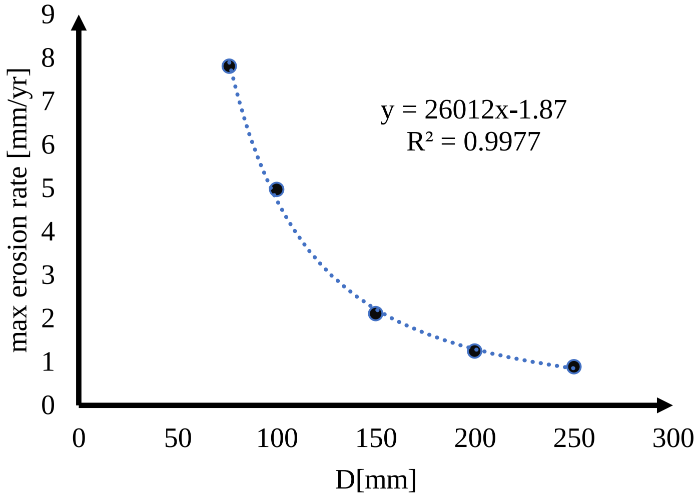

Figure 6. Effect of the pipe diameter on the maximum erosion rate for a 90° elbow

3.5.2. Bend angle

As explained, six bend angles including 45°, 60°, 90°, 120°, 135° and 180° have been modeled in the vertical position. The effect of the bend angle on the maximum erosion rate at the velocity of the inlet fluid flow of 11 m/s and particles size of 150 μm has been studied and presented in figure 7. According to the results, the maximum erosion rate increases with an increase in the bend angle from 45° to 90°. As the bend angle increases from 90° to 180° (from straight bend to sharp bend), a significant change has not been observed in the maximum erosion rate, and the erosion rate decreases slightly after the bend angle of 90°.

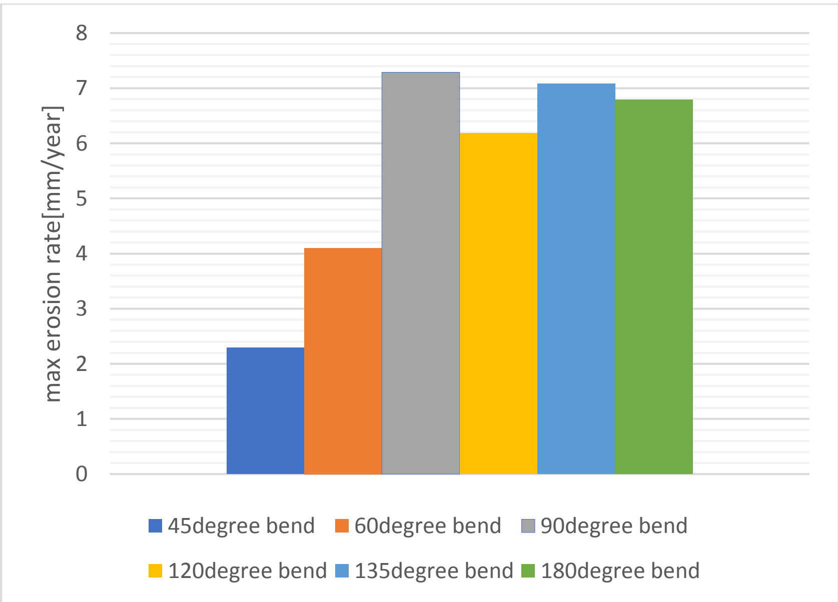

Figure 7. Effect of the bend angle on the maximum erosion rate inside pipes (the particles size of 150 μm and a flow inlet velocity of 11 m/s)

For further investigation, Figure 8 shows the predicted average erosion rate inside the pipes under the same conditions.

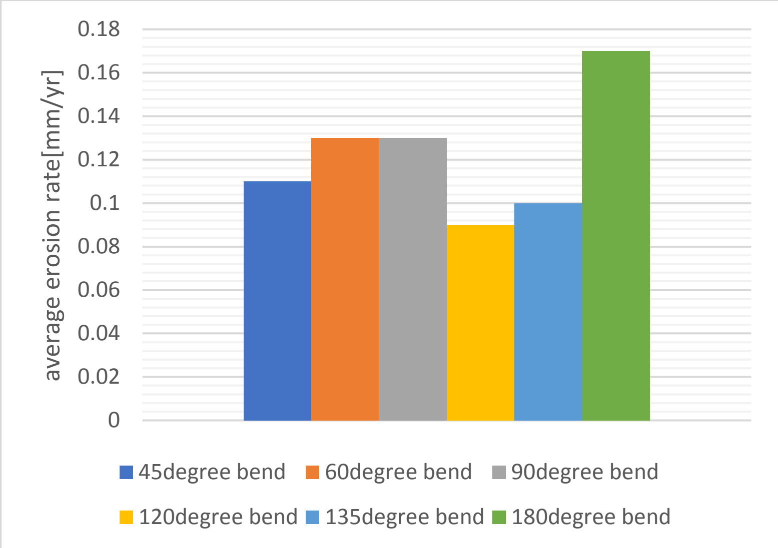

Figure 8. Effect of the bend angle on the average erosion rates inside pipes (the particles size of 150 microns and a flow inlet velocity of 11 m/s)

As it can be seen in the figure, the average erosion rate is almost the same for bend angles of 45°, 60°, and 90° (it is slightly lower for the 45° angle). the average erosion rate in the 120° and 135° bend angles almost has the same range and slightly (approximately 20%) lower than the previous bend angles (45°, 60°, and 90°) because of the wider area of collision on the wall surface. Finally, the 180° bend angle showed the highest average erosion rate (about two times that of 120° and 135° acute bends, and about 30% greater than that of the 90° angle bend). In this pipe, there are two large areas where the mass of particles efficiently collided the wall.

3.5.3. Pipe orientaion

All of the considered pipes with different bend angles were located vertically. This was so that gravity acted on the entrance straight section of the pipe before the bend in the opposite direction of the flow. To investigate the effects of the vertical and horizontal pipe positioning, the CFD simulation of the flow and prediction of the erosion rate inside the 90° elbow was conducted under the horizontal condition and the results were compared with the previous results of the vertical position. Similar to in the vertical position, the simulations of the flow in the horizontal pipe were performed at the inlet velocity of 11 m/s and particle size of 150µm. The predicted erosion rate in the vertical and horizontal 90° bend are presented in figure 9. The maximum predicted erosion rates are 7.3 and 14.6 mm/year for the vertical and horizontal bends, respectively. CFD results show a double increase in the maximum erosion rates for horizontal elbows as a result of asymmetrical particle collisions with the pipe wall. The Erosion distributions for the 90° vertical flow are almost symmetric, while the erosion distributions for 90° horizontal elbows are completely asymmetric.

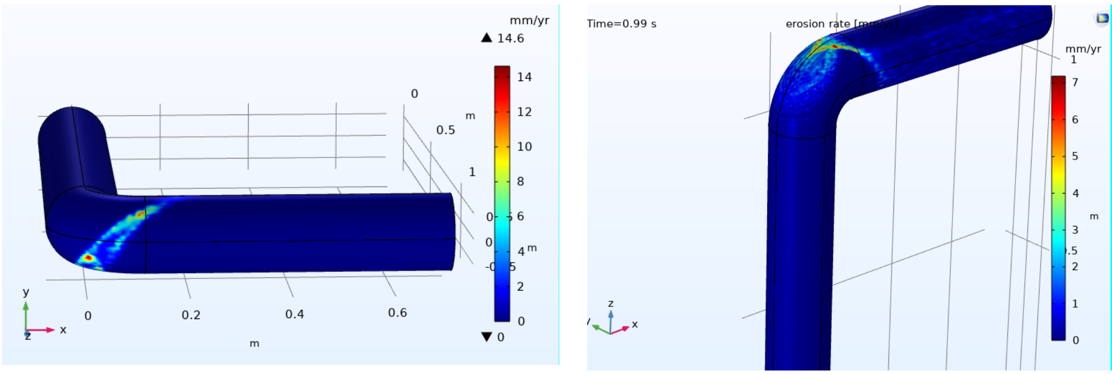

Figure 9. Comparison of the maximum predicted erosion rate in the horizontal and vertical 90° bends

3.6. Prediction of the possible leakage area

After a certain period of time, the erosion of the pipe surface causes the leackage particularly at the bend junctions. As a result of the CFD simulation, it is possible to identify the leakage area of the pipe, since the pipe leakage happens in the most eroded area of the pipe. The point of the leakage is the first point on the pipe that becomes damaged in the shortest period of time. The detection of pipe leakages is essential for preventing losses and reducing costs. Figure 10 shows areas with the potential leakage in 90° and 180° bends. In the 90° elbow, it is evident that the area of leakage is V-shaped. While, there are two areas with a high erosion rate in the 180° bend. Considering these two areas as the potential leakage areas, special attention should be paid to them. Upon impacting the first part of the bend, the particles are raised at a certain angle and continue to hit the end of the bend, increasing the erosion rate. For this bend, there are two areas susceptible to the fluid leakage.

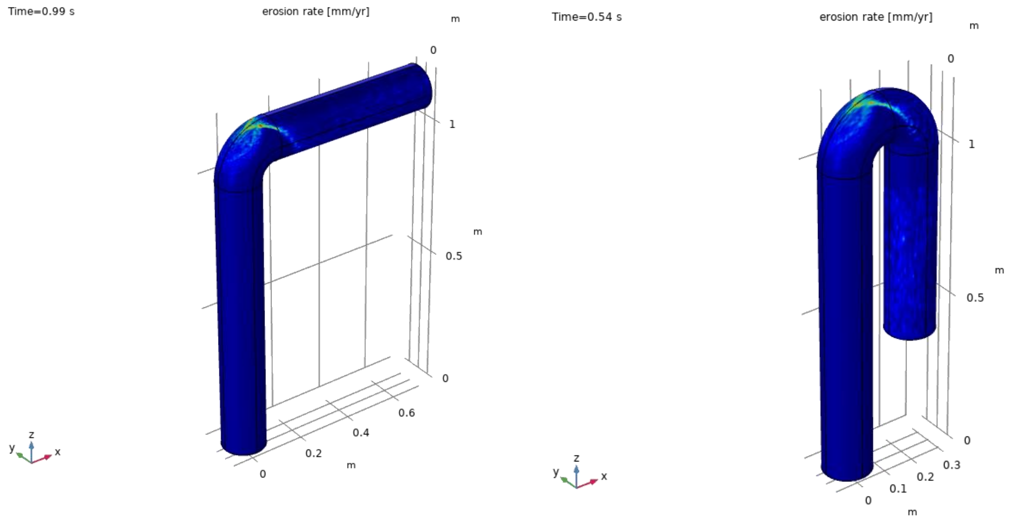

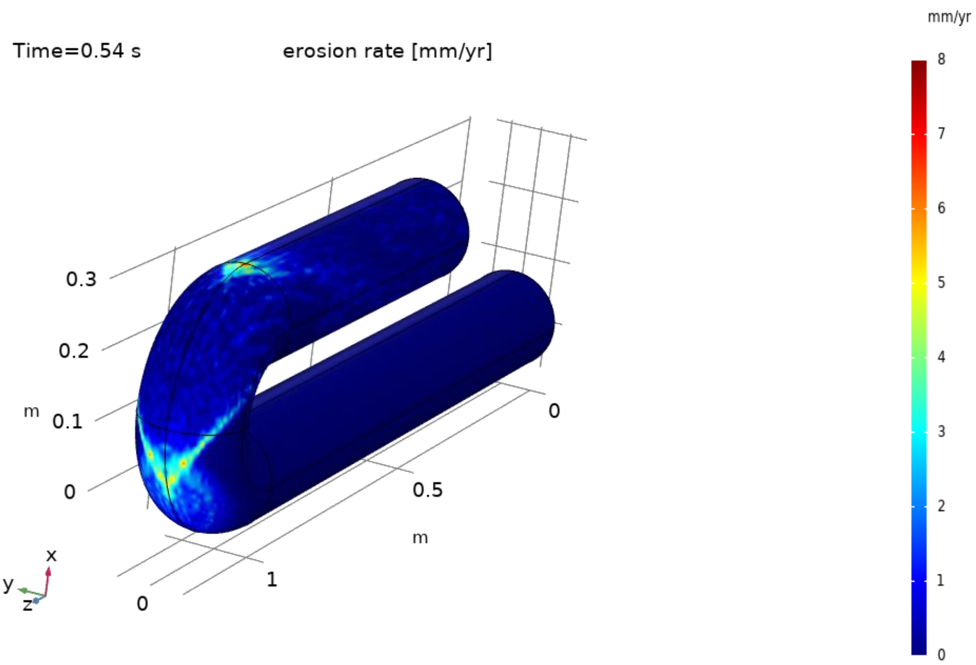

Figure 10. Areas of the potential leakage in the bends of 90° and 180°

3.7. Erosion rate along the pipe

It is important to analyze the erosion rate along the pipe as it provides detailed information about areas with high erosion rates. Figure 10 shows the erosion rate along the outer arc of the pipe curvature for the inlet velocity of 11 m/s and the particle size of 150μm. It is evident that the erosion rate varies along the arc, which is due to the fact that different areas receive different amounts of the shear impact energy. The shear impact energy is relatively low on the inner wall of the curve near the bend entrance, so the erosion rate is low at the entrance of the bends. For the bends of 45° and 60°, due to the higher particle speed at the end of the bend, the erosion rate is higher at this area. Thus, there is also a greater impact momentum, as well as more particles reaching the surface in this area. As the bend angle increases, the maximum erosion area becomes closer to the center of the bend. In the 120° bend, the maximum erosion rate takes place almost near the center. It was observed that the pipe with a 180° bend has two areas with high erosion rates, one in the first half of the bend and one at the end.

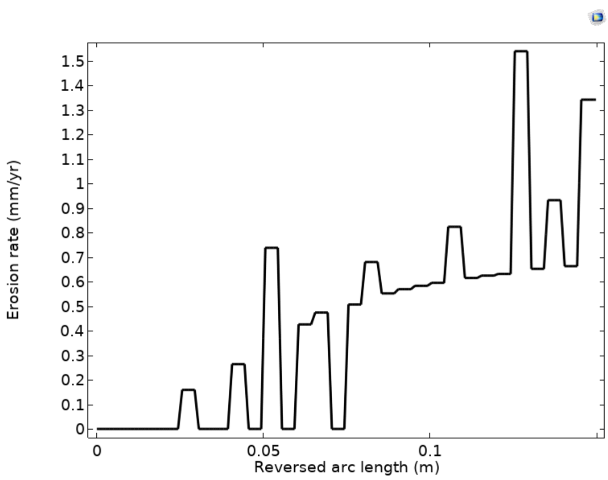

a) 45°bend

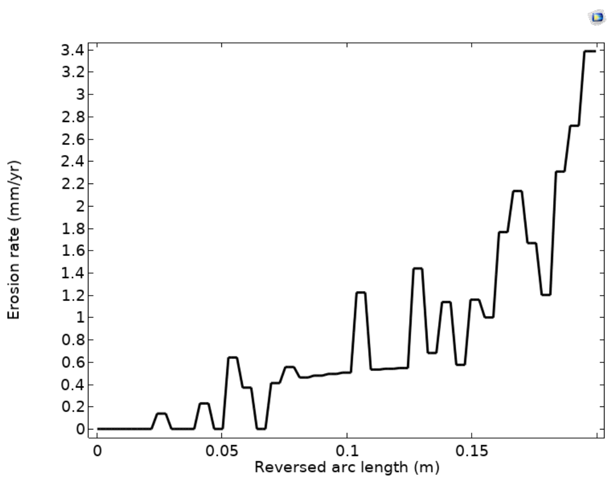

b) 60°bend

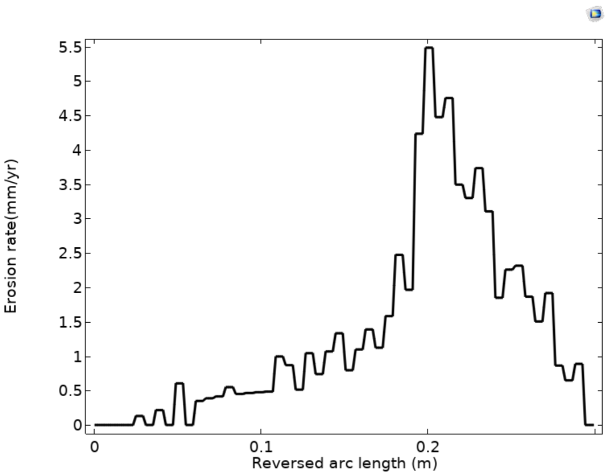

c) 90° bend

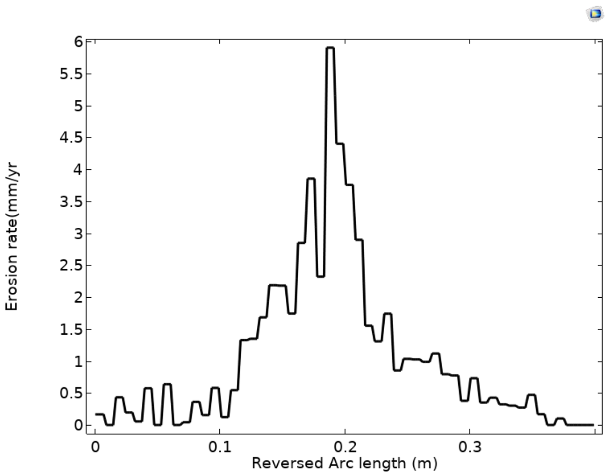

d) 120° bend

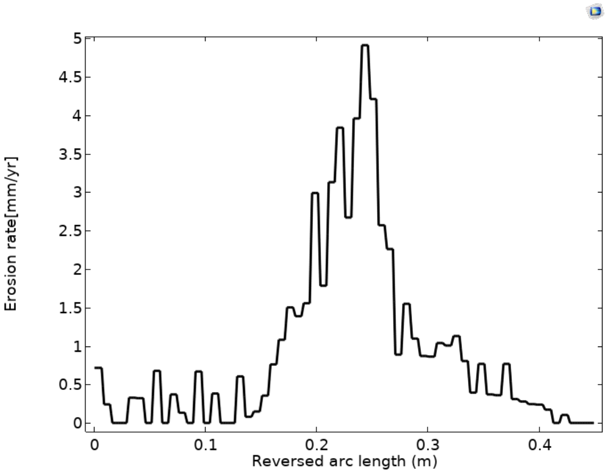

e) 135° bend

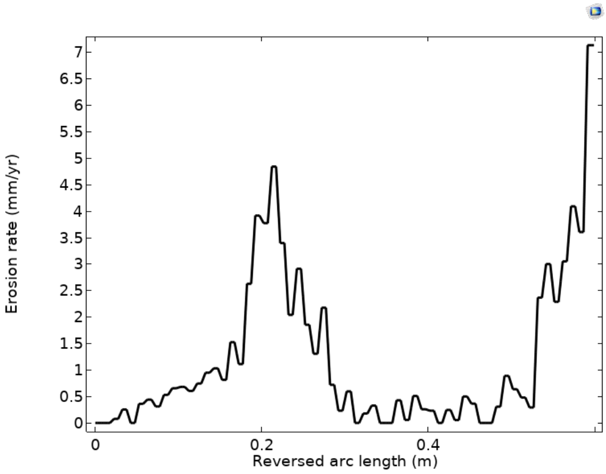

f) 180° bend

Figure 11. Predicted erosion rate in the outer arc of the pipe curvature

4. Conclusion

Due to the importance of the flows containing solid particles and the destructive effects of solid particles on various equipment, the prediction of the areas with the potential of damage are of great importance. This study was focused on the effect of bend angles on the flow hydrodynamics and the erosion rates. Computational fluid dynamics (CFD) were used to simulate the continuous fluid flow with solid particles as well as erosion phenomena within a pipeline. Different bends with curvature angles of 180°, 135°, 120°, 90°, 60° and 45° were considered and the air-sand flow with the inlet flow velocity of 11 m/s and the particle size of 150μm inside the pipe was modeled. For predicting the erosion rate in the pipe, in addition to the fluid flow governing equations, the E/CRC erosion model was used. In addition to the maximum erosion rate and average erosion rate, the areas with higher potential for leakage and damage were also predicted. These results are very useful for the repair and maintenance of the pipe wall.

References

[1] H. Y. Tang, H. C. Y. Foo, I. S. Tan, and M. K. Lam, "Photogrammetry based computational fluid dynamics of erosion of sand particles in water pipeline: Dynamic shape factors of 3D particles and minimization of erosion activity," *J. Pet. Sci. Eng.*, vol. 205, no. September 2020, p. 108794, 2021, doi:

10.1016/j.petrol.2021.108794.

[2] C. J. Ejeh, E. A. Boah, G. P. Akhabue, C. C. Onyekperem, J. I. Anachuna, and I. Agyebi, "Computational fluid dynamic analysis for investigating the influence of pipe curvature on erosion rate prediction during crude oil production," *Exp. Comput. Multiph. Flow*, vol. 2, no. 4, pp. 255–272, 2020, doi: 10.1007/s42757-019-0055-5.

[3] F. S. Bilal, T. A. Sedrez, and S. A. Shirazi, "Experimental and CFD investigations of 45 and 90 degrees bends and various elbow curvature radii effects on solid particle erosion," *Wear*, vol. 476, no. December 2020, p. 203646, 2021, doi: 10.1016/j.wear.2021.203646.

[4] G. C. Pereira, F. J. De Souza, D. Alves, and D. M. Martins, "Numerical prediction of the erosion due to particles in elbows," *Powder Technol.*, vol. 261, pp. 105–117, 2014, doi: 10.1016/j.powtec.2014.04.033.

[5] W. Jia, Y. Zhang, C. Li, P. Luo, X. Song, and Y. Wang, "Journal of Natural Gas Science and Engineering Experimental and numerical simulation of erosion-corrosion of 90 ◦ steel elbow in shale gas pipeline," vol. 89, no. January, 2021.

[6] O. Ayala and C. Knight, "Computational Fluid Dynamics Study of the Effects of Secondary Flows in 90- degree Pipe Elbow Erosion," vol. 11, pp. 1–4.

[7] P. Zahedi, M. Parsi, A. Asgharpour, B. S. Mclaury, and S. A. Shirazi, "Experimental investigation of Sand Particle Erosion in a 90 ° elbow in Annular Two-Phase Flows," *Wear*, p. 203048, 2019, doi: 10.1016/j.wear.2019.203048.

[8] C. J. EJEH and G. P. AKHABUE, "Computational Fluid Dynamics Analysis on Pipeline Erosion due to the Presence of Solid Particles.," *All Nations Univ. J. Appl. Thought*, vol. 6, no. 2, pp. 189–215, 2019.

[9] S. Yang, M. Zhang, X. Wang, and H. Wang, "Numerical Simulation of Fluid Carrying Pollutant Particles Erosion in Elbow Pipe Is Carried out by COMSOL," in *Journal of Physics: Conference Series*, 2020, vol. 1626, no. 1, p. 12109.

[10] X. Chen, B. S. Mclaury, and S. A. Shirazi, "Application and experimental validation of a computational fluid dynamics (CFD) -based erosion prediction model in elbows and plugged tees," vol. 33, pp. 1251–1272, 2004, doi: 10.1016/j.compfluid.2004.02.003.

[11] W. S. Khur and Y. Y. Jian, "SC," *J. Pet. Sci. Eng.*, 2019, doi: 10.1016/j.petrol.2019.01.001.

[12] R. E. Vieira, A. Mansouri, B. S. McLaury, and S. A. Shirazi, "Experimental and computational study of erosion in elbows due to sand particles in air flow," *Powder Technol.*, vol. 288, pp. 339–353, 2016, doi: 10.1016/j.powtec.2015.11.028.

[13] J. Yan, A. Korobenko, A. E. Tejada-Martinez, R. Golshan, and Y. Bazilevs, "A new variational multiscale formulation for stratified incompressible turbulent flows," *Comput. Fluids*, vol. 158, pp. 150–156, 2017.

[14] E. C. Jekwu, A. G. Precious, and A. B. Evans, "Evaluating the impact of unsteady viscous flow and presence of solid particles on pipeline surfaces during crude oil transport," *Acta Mech. Malaysia*, vol. 2, no. 2, pp. 20–27, 2019.

[15] I. Finnie, "An experimental study of erosion," *Proc. Soc. Exp/Stress. Anall*, vol. 17, no. 2, p. 65, 1960.

[16] Y. I. Oka, K. Okamura, and T. Yoshida, "Practical estimation of erosion damage caused by solid particle impact Part 1 : Effects of impact parameters on a predictive equation," vol. 259, pp. 95–101, 2005, doi: 10.1016/j.wear.2005.01.039.

[17] D. N. Veritas, “Erosive wear in piping systems–recommended practice RP O501,” *Det Nor. Verit.*, 1996.

[18] G. F. Homicz, “Computational Fluid Dynamic simulations of pipe elbow flow.,” Sandia National Laboratories (SNL), Albuquerque, NM, and Livermore, CA …, 2004.

[19] R. E. Vieira, M. Parsi, P. Zahedi, B. S. McLaury, and S. A. Shirazi, “Ultrasonic measurements of sand particle erosion under upward multiphase annular flow conditions in a vertical-horizontal bend,” *Int. J. Multiph. Flow*, vol. 93, pp. 48–62, 2017, doi: 10.1016/j.ijmultiphaseflow.2017.02.010.